Electric Vehicle Battery Cell Cycle Aging in Vehicle to Grid Operations: A Review

Timo Lehtola, *Student Member, IEEE,* Ahmad Zahedi, *Senior Member, IEEE,*

***Abstract*—Electric vehicle owners need vehicle to grid operations information before being able to participate in power grid support. Specifically, the lack of understanding of the effect of battery charge and discharge on the lifetime of battery cells inhibits full participation. Batteries are expensive, but increasing their lifetime is one solution to reduce costs. Several battery aging models have been developed to calculate the lifetime and cost of vehicle to grid operations. This review contributes to what is already known by connecting measurement data, driving data, and vehicle to grid operations to the battery cycle aging model. The review identified time, temperature, and the state of charge influence calendar aging. In addition, a number of cycles, depth of discharge as well as charging rate influence cycle aging. Results indicated the batterys naturally decreasing lifetime can be reduced and scheduled charging can extend lifetime. The implications of vehicle to grid operations on battery durability plays an important role in the convenience for electric vehicle owners to support the power grid with ancillary service contribution.**

***Index Terms*—Aging, batteries, computational modeling, control systems, degradation, economics, electric vehicles, electrodes, energy management, equations, estimation, frequency control.**

I. Introduction

ELECTRIC VEHICLE (EV) batteries are used for Vehicle to Grid (V2G) operations, driving, powering electronics, or other purposes. The vehicle owner can affect battery life, either by driving or V2G operation. As the purpose of EV is driving, it does not make sense to radically change driving patterns. Thus, controlling battery usage for V2G operations is preferred. V2G operations reduce battery cycle lifetime (the number of times the battery can be recharged to its full capacity reveals battery lifetime [1]), and reduced lifetime is a cost for battery owners. Additionally, annual driven distance and the number of V2G cycles also increase V2G cost. As vehicle owners will probably vary greatly in the level of V2G operation participation, from total to no participation, vehicle owners will need information on how charging and discharging patterns manage battery aging in V2G operations.

Build factors that affect battery life include the battery type and the number and the quality of battery cells used. The EV driver factors that affect battery life include control over the accelerator pedal, the driving schedule, and determining energy consumption and battery State of Charge (SoC) evolution [2]. In general, battery durability declines further into a batterys life and as a function of the number of charges and discharges it has gone through.

In V2G operations, EV batteries provide i) power supply for EV propulsion and ii) improve electricity grid stability. These dual uses will result in increased degradation of the EV batteries. The SoC of the battery expresses the level of electrical charge in the EV battery cell. However, EV operators affect battery life by storing the batteries at different SoC levels [3]. As a result of a reduced lifetime, battery wear should be considered as a part of the economic evaluation [4]. As EV owners have battery degradation cost due to V2G operations, the EV owner needs to consider V2G cost as a part of the operational cost and battery replacement cost.

This review connects all the considered methods: measurements, cycle life models, daily driven patterns, calculating lifetime and driving distance, and V2G operations, to a battery cycle aging model. The battery model is useful for EV battery management systems to enhance the cycle life of EV batteries. The novelty of this review is the consideration of charge limits according to driving distance. The model optimizes charging and discharging and calculates an approximation of a batterys life cycle.

An outline of this review is as follows

- I Introduction
- II Methodology
- III Aging tests
- IV Battery chemistries examined in cycle life studies
- V Cycling experiments
- VI Configuration for the battery model
- VII Battery cell aging tests
- VIII Validation of battery aging model
- IX Interpretation and discussion
- X Conclusion

II. Methodology

A literature search was done for battery calendar aging and cycle aging studies. The identified cycle life studies were divided according to battery chemistry and study methods. Most of the reviewed studies carried out battery cell aging tests [5]–[72].

Accelerated battery cell aging measurements from [11] were used to construct a cycle aging model. Battery cell tests were carried out with several measurements [11]. The battery charge was at an average SoC of 50% [11]. The aging level was recorded several times during measurements [11].

Driving data [73] showed demand for equivalent full cycles. The proposed V2G cycles will draw 5% of battery energy in time to keep battery cells in an optimal charging area [11].

This research work was in part supported by the College of Science and Engineering and the Graduate Research School, James Cook University, Australia. (Corresponding author: Timo Lehtola).

T. Lehtola and A. Zahedi are with the College of Science and Engineering, James Cook University, Queensland, Australia (e-mail: timoantero.lehtola@my.jcu.edu.au; Ahmad.Zahedi@jcu.edu.au).

Aging data shows the number of cycles during the lifetime. Lifetime cycles can be transformed to driving distance using range information from EVs [71]. As a result, the full driving distance is divided by average annual distance answering the question of how long should batteries last in V2G operations [71].

III. Aging tests

V2G operations have the capacity to solve problems in the power grid and battery cell aging. Power grid uncertainties, including load demand variation, renewable generation fluctuation, energy price and failure of generators is possible with grid support [74]. Demand response simulations provide frequency control to the power system [75]. Decentralized control strategies dominate renewable energy electricity networks [76]. With time and battery cell use, Lithium-ion (Li-ion) battery cells experience capacity performance degradation, commonly called aging. The aging occurs because of time, temperature, level of SoC, a number of cycles, Depth of Discharge (DoD) level as well as charging rate [77]. Fast charging is a problem because it pumps energy to the battery faster than the expected speed of chemical reaction [78]. This may influence local overcharge reactions, such as polarization and overheat. However, a short discharge pulse during the charge rest period depolarizes the cell, and this normalizing of the ion concentration enhances battery life [78]. High currents in fast charging can be mitigated by using ultracapacitors [79]. The control system mitigates small transient disturbances to enhance battery life [80]. Chemical reasons in the aging processes are lithium deposition, the formation of passive films, crack propagation as well as an active lithium dissolution in the electrode [77]. To mitigate battery degradation in V2G process, a Li-ion battery model showed that delayed charging and V2G reduced the average SoC [81]. The mitigating result was a battery life of 7.2 years before it reached 80% SoC of initial battery capacity [81]. This means that a battery cell charged up to 100% of its SoC has 80% capacity [81].

The objective of the current review was to use the battery cell aging model [71] to calculate how many years battery cells last in V2G process under normal driving patterns. In this model, the optimal charging procedure chooses optimal charge limits according to the driving distance of that day. In V2G operations, three major categories of controllable load capabilities are energy storage, shifting, and curtailment capability [74]. In V2G operations, EV battery storages are small energy storages. Cycling tests for $LiFePO_4$ batteries demonstrated that $LiFePO_4$ battery cells are not overly sensitive to the DoD as are many other Li-ion batteries [53]. This means that EVs can use a higher proportion of batteries and can survive with smaller battery capacity. Battery capacity refers to the maximum battery capacity that the battery cell can deliver from a full discharge process. When battery capacity is fading, the fading should be calibrated after cycles by standard capacity tests, which are made under standard rate and temperature [53].

Laboratory experiments and Reference Performance Tests (RPT) have been conducted on $LiFePO_4$ cells, providing a method towards early lithium plating detection [82]. The cycling experiments with $Li(NiMnCo)O_2$ battery cells indicated that cycling around a mean value of 50% provides the longest battery cell lifetime [11]. For instance, the cycles between 47.5% and 52.5% of SoC allowed the longest lifetime of 8,500 cycles. In contrast, the full area cycles between 0 and 100% of SoC allowed the shortest lifetime of 440 cycles before cells reached 80% of the cell capacity [11]. An equivalent full cycle is several partial charges, which equates to one full charge. For example, in a 500 km range, 300 km and 200 km partial charges develop one equivalent full cycle. To ensure a longer lifetime, batteries should recharge after batteries have less than 50% SoC charge because large cycle depths increase battery cell aging [11]. However, over time, batteries naturally show poor performance [11]. During cycle aging tests, after cells reached 80% of the original capacity they began to have sudden deaths [11]. The implication is that battery cells become unreliable after cells reach 80% of the original capacity. However, on second-life battery applications, battery cells are still operational after reaching 80% capacity [83]. In addition, a 400 day battery storage test demonstrated that empty batteries had the weakest capacity fading while full batteries had the strongest capacity fading [11]. Also, an aging test with $Li(Ni_{1/3}Mn_{1/3}Co_{1/3})O_2$ illustrated that the longest lifetime area was 30-50% SoC [27], which was slightly under the optimal 50% SoC for $Li(NiMnCo)O_2$ batteries [11].

IV. Battery chemistries examined in cycle life studies

EV battery materials are based on lithium combined with other metals. Table I lists several Li-ion battery chemistries which could be considered for EV applications. Some are under high research interest, while others are conceded as less promising for EV applications [84]. Examined cycle life studies include various applications of batteries in addition to electromobility applications.

The primary interest of the EV industry particularly concentrates life cycle studies on $LiFePO_4$ (LFP) and $LiNi_xCo_yMn_zO_2$ (NCM or NMC), commonly known as $Li(Ni_{1/3}Mn_{1/3}Co_{1/3})O_2$, battery chemistry. Only a few studies have used $LiMnO_2$ (LMO), $Li_2Mn_2O_4$ (also LMO), $LiCoO_2$ (LCO), $LiNi_{0.8}Co_{0.15}Al_{0.05}O_2$ (NCA) or $LiNi_{0.8}Co_{0.2}O_2$, which indicates fewer EV applications in the near future. Only one cycle life study has been performed with $LiNiO_2$ (LNO) and with $Li(Ni_{0.5}Mn_{0.5})O_2$ (NMO), and another form of NMO, $LiNi_{0.5}Mn_{1.5}O_4$ [85]. However, how other materials can be adapted to EV applications is not yet known. Materials, those currently not actively researched, include Li_2TiO_3 (LTO), $LiCoPO_4$ (LCP), $LiFeSO_4F$ (LFSF) and $LiTiS_2$ (LTS). Additionally, cathodes $LiMnPO_4$ (LMP), $LiNi_{0.5}Co_{0.5}PO_4$, (NCP), $LiMn_{1/3}Fe_{1/3}Co_{1/3}PO_4$ (MFCP) and $Li_3V_2(PO4)_3$ (LVP) (see Table II). These other chemistries are not intensively studied because EV battery chemistries have different performance characteristics, limitations, and development breakthroughs.

Battery cell wear decreases battery capacity, increases inner resistance, increases power loss, and causes a variation in

TABLE I
LI-ION BATTERY CHEMISTRIES CONSIDERED FOR ELECTRIC VEHICLE APPLICATIONS

Abbreviation	Name	Chemical formula
LCO	Lithium Cobalt Oxide	$LiCoO_2$
LCP	Lithium Cobalt Phosphate	$LiCoPO_4$
LFP	Lithium Iron Phosphate	$LiFePO_4$
LFSF	Lithium Iron Fluoro Sulphate	$LiFeSO_4F$
LMO	Lithium Manganese Oxide	$LiMnO_2$ or $Li_2Mn_2O_4$
LMP	Lithium Manganese Phosphate	$LiMnPO_4$
LNO	Lithium Nickel Oxide	$LiNiO_2$
LTO	Lithium Titanium Oxide	Li_2TiO_3
LTS	Lithium Titanium Sulphide	$LiTiS_2$
LVP	Lithium Vanadium Phosphate	$Li_3V_2(PO_4)_3$
MFCP	Lithium Manganese Iron Cobalt Phosphate	$LiMn_{1/3}Fe_{1/3}Co_{1/3}PO_4$
NCA	Lithium Nickel Cobalt Aluminium Oxide	$LiNiCoAlO_2$
NCM or NMC	Lithium Nickel Cobalt Manganese Oxide	$LiNi_xCo_yMn_zO_2$
NCP	Lithium Nickel Cobalt Phosphate	$LiNi_{0.5}Co_{0.5}PO_4$
NMO	Lithium Nickel Manganese Oxide	$Li(Ni_{0.5}Mn_{0.5})O_2$

TABLE II
CONSIDERED CONTEMPORARY CYCLE LIFE STUDIES

Positive electrode (cathode) material	Cycle life studies*
$LiMn_2O_4$	[12], [14], [16], [24], [30], [32]–[34], [56], [65], [72]
$Li(NiMnCo)O_2$ or $Li(Ni_{1/3}Mn_{1/3}Co_{1/3})O_2$	[11], [12], [16], [19]–[21], [27], [29], [30], [32], [33], [35], [41], [44], [46], [51], [56], [65], [89]
$LiCoO_2$	[14], [31], [67]–[69]
$LiNiO_2$	[85]
$LiNi_{0.8}Co_{0.15}Al_{0.05}O_2$	[28], [51], [90]–[95]
$LiNi_{0.8}Co_{0.2}O_2$	[49], [96]–[101]
$LiFePO_4$	[6]–[8], [10], [14]–[16], [18], [23]–[26], [28], [36], [37], [42], [44], [45], [48], [50], [52], [53], [56], [57], [59], [61]–[66], [72], [102], [103]
$LiNi_{0.5}Mn_{1.5}O_4$	[104]

*For more detail, please refer to the cycle life studies references.

impedance spectra [86]. Battery cell wear also depends on temperature, DoD and charging and discharging power [86], [87]. Control of battery temperature is a vital part of an EV battery management system [88]. Degradation causes and outcomes were modeled [77]. Several aging tests, which have been carried out with different cathode materials, are identified in Table II.

A. $LiMn_2O_4$ cell aging

$LiMn_2O_4$ cell aging tests detected capacity fade as well as an increase of inner resistance. The main reason may be thermal processes, which are linear with time [12]. Health monitoring methods have been developed to estimate battery SoC [105], [106]. One research [14] developed improved health monitoring methods' capacity model based on the battery cell charging and discharging processes. The anode impedance increased manganese dissolution on carbon anodes [14]. This was not found in Li_2TiO_3 material, which has a negligible Solid Electrolyte Interface (SEI) growth [16]. External aging reactions accelerated the aging, including SEI growth, loss of active material, and Li-ion plating [30]. An experiment cycled Li-ion cells between 10% and 100% of SoC [32]. Increased cycle numbers resulted in an increase in the cathodes resistance. This increase was particularly visible for a 10% SoC and a 100% SoC.

Aging tests [33] studied the dependence of battery cell degradation and aging. The presented aging model synthesized various cell degradation methods, such as loss of active lithium, loss of lithium inventory, an increase of polarization resistance, the parasitic phase formation, and lithium plating. After 120 days of operation, cells were tested and the internal resistance increase was lower than 1%. The explanation could possibly be a) lithium insertion or b) extraction processes that in turn influence mechanical fracture of active particles [34]. A battery degradation model [56] was presented since the model smoothly integrates into the energy exchange simulation and estimates the battery cell aging. Generally, it can be stated that $LiMn_2O_4$ chemistry is a promising battery type for future transportation [65].

B. $Li(NiMnCo)O_2$ cell aging

In $Li(NiMnCo)O_2$ aging tests [19], incomplete stripping of lithium as an effect of the SEI growth was described. The SEI growth may lead to an effective loss of lithium metal on model substrates [19]. One study [21] investigated the capacity degradation mechanisms of $LiNi_{0.6}Co_{0.2}Mn_{0.2}O_2$ cells. The main reason for cell capacity degradation was the loss of active material due to the SEI layer formation, which combined with the degradation of the electrode. An investigation [41] of the calendar aging behavior of Li-Ion cells with NMC cathode and cycle aging at several temperatures and SoCs was able to obtain estimations of capacity loss from the capacity and resistance model, and validate the model with measurements. Low earth orbit simulations [107] revealed the cycle aging using a physics-based model.

C. $Li(Ni_{1/3}Mn_{1/3}Co_{1/3})O_2$ cell aging

In $Li(Ni_{1/3}Mn_{1/3}Co_{1/3})O_2$ aging tests, the capacity degradation rate influenced the EV range as well as decreased the discharge capacity during V2G operations [44]. This understanding enables us to establish a quantitative physical model. This model describes the cell aging process for NMC cells with variance in battery cell aging due to power pulses and thermal cycling [89]. An alternative approach would be that increased capacity superimposes SEI formation [20]. For battery aging prediction, many aging characteristics, such as temperature, storage voltage, time, cycle depth, SoC, electric current as well as charge throughput have been accounted [20]. By monitoring the characteristics of SoC, capacity, impedance, power, State of Health (SoH) as well as estimated life, and the calendar and cycle life experiments indicated that lower

temperatures resulted in a longer lifetime [29]. The challenge was that most battery cell characteristics, including battery capacity and impedance characteristics, varied significantly due to aging [35]. The metallic lithium plating on the electrode was the main reason for the batterys collapse [46]. An exponential function has been used to calculate the calendar capacity fade [51]. For $Li(Ni_{1/3}Mn_{1/3}Co_{1/3})O_2$ tests, the lowest test temperature was 25 °C and the lowest test storage charge was 20% SoC, revealing the longest life [20]. Calendar aging for $Li(NiMnCo)O_2$ showed that empty cells survived longest, and cells cycled between 45% and 55% SoC offered the longest lifetime [108].

D. $LiCoO_2$ cell aging

$LiCoO_2$ aging tests [13] highlighted that the change in the current rate changes the capacity fade. The higher rates of current accelerated the deterioration of Li-ion electrodes [13]. A capacity analysis used a single cell equivalent circuit model [109]; however, it was difficult to precisely determine the SoC [109]. The incremental capacity analysis identified the capacity loss for battery cells [109]. In addition to capacity and resistance characteristics, aging studies also focus on equivalent circuit analysis in cycle aging [110] and in calendar aging [111]. The SoC had a neglecting effect on capacity degradation when the charge voltage was below 3.92 V [112]. However, increased charge voltage increased the rate of capacity degradation. The capacity degradation rate is independent of the SoC when SoC is lower than 50% [112]. Therefore, battery cell aging decreases battery energy capacity [31].

Stack stress evolution is considered a dynamic quantity during battery cell aging. As a result of electrode charging strains, stack stress fluctuates with SoC and gradually accumulates over the cell aging [67]. One study [69] reported that the mechanical and phase changes of the cathode. The negative influence of the root mean square value of charge and discharge currents, Alternating Current (AC) waveform shape, AC frequency and root mean square current amplitude increased battery aging [113].

E. $LiNi_{0.8}Co_{0.15}Al_{0.05}O_2$ cell aging

Cycle aging tests with $LiNi_{0.8}Co_{0.15}Al_{0.05}O_2$ cells studied cell performance and pulse power capability. Room temperature measurements at 100% DoD led to faster capacity degradation and increased impedance, compared to measurements at 70% DoD [93]. High temperatures from 40 to 70°C increased SEI growth and generated micro-cracks at grain boundaries causing capacity fade [114]. The RPT tests, including constant current, constant power, variable power, and peak power tests, have confirmed consistent temperature [109]. The differential voltage analyses [115] indicated that the capacity degradation was due to chemical reactions at the anode. Differential voltage dV/dQ curves visualized reactions at the anode [116].

Since battery behavior changes due to aging, the design of sophisticated battery management can provide longevity and performance [117]. Capacity fade in a 22 month calendar aging test was 4% at 40 °C [90]. In a hybrid EV study, a load profile maintained 60% SoC [28]. The capacity degradation was included in an empirical cycle aging model [28]. However, this empirical aging model was not able to reveal the degradation mechanism. A load profile was developed to study the degradation mechanism with LFP and LMO + NMC batteries [72]. Lithium Nickel Metal Oxide $Li[Ni_{1-x}M_x]O_2$ cells have a high capacity, high discharging rate and relatively low cost [92], [94]. However, these battery cells have a limited lifetime, especially at high temperatures. This is why this battery chemistry is not available for commercial use [92], [94].

F. $LiNi_{0.8}Co_{0.2}O_2$ cell aging

In $LiNi_{0.8}Co_{0.2}O_2$ aging tests, one research presented experiments and an aging model for battery cells [96]. The research also included experiments with $LiNi_{0.8}Co_{0.15}Al_{0.05}O_2$ battery cells, investigating and validating the results with a test matrix. Impedance tests determined that the main contributor to battery cell impedance rise is a cathode impedance [97]. A capacity fade, impedance rise, potential change, SoC and SoH are electrochemical variables, which can be monitored for battery calendar aging [98]. Gravimetric energy density and battery cycle aging are important factors for aerospace Li-ion cells and batteries [49]. The SEI growth causes an internal impedance rise [96]. Therefore, the model was constructed with exponential functions to reveal the impedance rise [96].

G. $LiFePO_4$ cell aging

In $LiFePO_4$ aging tests [102], storage temperature conditions of 30, 45, and 60 °C and storage conditions of 30, 65, and 100% SoC, the battery degradation was faster with the temperature than with the SoC. The main reason for the degradation mechanism was the loss of lithium inventory due to the SEI growth [118]. SoC, temperature, and It-rate contribute to battery cell aging and are included in the LFP cell aging model [23]. It-rate means discharge current related to capacity; in a 2 Ah battery discharged in a 2 A current means an It-rate of 1. The electrical load was analyzed and analytical impedance spectroscopy was used to build the LFP battery model [119]. The main reason for aging is a loss of active form of lithium. Firstly, metal-ions on the anode react with the electrolyte and dissolve in the electrolyte. Secondly, electrolyte reacts with the cathode. Finally, SEI film reduces active Li-ions in the cathode [120]. A new fast-charging method for LFP was introduced [37]. The SEI growth on particle surfaces causes particle disconnections. In turn, this increases material resistance and causes capacity degradation [121].

A study [66] presented a genetic resampling particle filter method to estimate SoH for a battery cell. Experiments [42] carried out on LFP cells at temperature conditions 25 °C and 60 °C showed an increase in LFP cell inner resistance. Inner resistance was five times higher at a temperature of 60 °C than a cell tested at 25 °C. The degradation process for LFP cells starts with the loss of lithium inventory. The next stage in the process combines loss of lithium inventory, loss of active lithium and degradation of kinetic reaction [15], which showed the main mechanism for aging during the first phase

of the degradation process is the loss of lithium. Thus, the loss of active lithium accelerates degradation, causing the End of Life (EoL) for cycle aging experiments [63]. The obtained results the lifetime of LFP cells is longer at low charging and discharging rates than at high charging rates [63]. Unwanted lithium plating is only observed when battery cells are charged and discharged in a narrow SoC window [61].

A circuitbased model for the SoH estimation of battery cells in EVs has been proposed [122]. The proposed aging model was based on coupling constant and various factors. One study [57] comprehensively considered factors for battery lifetime, including ambient temperature, charging and discharging rates as well as charging and discharging cut-off voltage as the input stresses. The influence of ambient temperature refers to the Arrhenius modeling method whereas the influence of electrical factors refers to an inverse power law relationship. The model analyzed the weights of the influence on the cell aging based on the sensitivity of the life model factors. The prediction error for the battery cell aging was under 15%. A study [62] proposed a diagnostic technique to indicate an SoH for Li-ion cells. This method analyzed measured voltage and current signals. The degradation process had a correlation to the special battery cell materials and to the manufacturing method of the cell [59].

A semi-empirical capacity fade model investigated and considered the contribution of temperature, cycle rate, and DoD [52]. The study results [45] introduced a circuit model that selects Li-ion cells randomly and separates these cells from the battery for SoH investigation. Another study [53] analyzed the business value of V2G operations for load management in a power grid. The received benefits need to exceed the cost of V2G operations. Considered benefits of V2G operations are, for example, providing peak power management or spinning reserve services. Considering the cost of V2G operations are EV battery capacity fade, V2G electronics and communication infrastructure, and energy production losses. In cell power performance fade, plated lithium loses its conductive connection to graphite by isolation [18]. The lithium lost may enhance the growth of the SEI layer, which deteriorates kinetics of the anode materials, in turn, enhances the lithium plating. This causes loss of the battery cell electrolyte because of a decomposition process, finally leading to the end [18]. One study [10] analyzed the influence of high ambient temperature on calendar capacity fade. The high ambient temperature and calendar aging induced extra battery aging and therefore, the main degradation process, loss of lithium, changed to a combined loss of lithium and loss of active lithium [10]. The loss of active lithium accelerates the battery cell performance fade.

The combination of calendar and cycle aging covers a wide range of combinations to form a cost-effective model for lifetime estimation [64], [123]. A study [26] indicated that the shallower the DoD, the more energy can be cycled before the cell reaches EoL. LFP chemistry provides a long calendar aging [50]. The cycle aging reached 8,000 cycles at room temperature. Power degradation under normal EV cycles was in the very low range, 3.275.59%. The reduction of EV range was mainly based on capacity fade rather than power degradation.

TABLE III
CONSIDERED METHODS OF THE PROPOSED APPROACH IN CONTEMPORARY CYCLE AGING STUDIES

Study method	Cycle aging studies*
Cycle aging measurements	[5]–[72]
Cycle aging models	[5], [6], [10]–[12], [14]–[21], [23], [26]–[28], [30], [35], [39]–[41], [43]–[45], [48], [50]–[52], [55]–[60], [62]–[64], [66], [70]–[72], [124], [125]
Daily driven patterns	[25], [34], [50], [53], [55], [58], [59], [71], [124]
Connect V2G operations to an aging model	[28], [43], [53], [55], [64], [70], [71], [126]
Calculated EV battery lifetime in years or calculated lifetime driving range	[11], [20], [27], [28], [34], [37], [54], [55], [60], [71]

*For more detail, please refer to the cycle life studies references.

A capacity degradation model [36] predicted aging at low SoC rates. After constructing the model, the experiments validated the model. Li-ion cells experience calendar aging and cycle life aging. The monitoring system for performance degradation can track the capacity fade and increase the inner resistance. In calendar and cycle aging, inner resistance increases because of contact losses and formation of resistive surface film behavior. Loss of Li-ions and active electrode material can influence capacity fade.

Both calendar and cycle aging depend on battery cell chemistry and operational conditions [6]. Operational conditions for calendar aging are temperature, SoC and time. Operational conditions for cycle aging are temperature, SoC, cycle number as well as charge and discharge voltage. High temperatures from 40 to 70 °C increased SEI growth and generate microcracks at grain boundaries. Lithium metal plating intensified at low temperatures. Increased cycle numbers will result in an increase in the cathodes resistance. High voltage can cause unwanted anode reactions and increase anodic currents. The higher rates of current accelerated the deterioration of Li-ion electrodes. Some aging factors come from the power grid, for example, peak current demand. These variables interact with each other, forming a complicated process for aging [6]. Therefore, models can estimate aging, and experimental tests provide figures that are more realistic. However, interactions may be difficult to understand and quantify [25]. The high conductivity and high tap density provide relatively low reactivity and high energy density to LFP cells [103]. EV batteries have similar lifetime expectations; however, differences come from technology, battery management, producer, and battery model. Several cycle aging measurements and cycle aging models exist. Some of these use daily driven patterns and connect V2G operations to that model [53], [55], [71]. In addition, some studies calculate EV battery lifetime in years or calculated lifetime driving range. Table III lists five methods used for cycle aging studies.

V. CYCLING EXPERIMENTS

Cycling experiments with the $LiNi_{0.5}Mn_{1.5}O_4$ electrodes involved an irreversible phenomenon: the measured charge

capacity stored by cells was higher than the available discharge capacity [104]. However, the cycling rate was It/16, which was lower than normal cycling rates for the commonly available EV charger rates. Therefore, slow charging with high voltage can cause unwanted anode reactions and increase anodic currents. The inner resistance rise and degradation of capacitance parametrization factors depend on the operational points of the cell: temperature, time, SoC, power demand and cell aging [5]. An experiment [9] on battery cells stressed with different charging and discharging rates estimated SoH and consequently the effects due to cell aging. The cell aging study revealed that either the DoD, which increased from 20% to 40% or the temperature, which increased from 25 °C to 45 °C, has a small impact on cell degradation and end of voltage. However, a simultaneous increase in DoD and temperature significantly increased degradation, as did the discharge rate, which was It/3 [127]. An investigation [22] predicting cycle aging of second-life battery applications discovered that the capacity retention as a function of cycle numbers agrees with a Gaussian function. In another cycle aging performance test [128], the cells subjected to a higher temperature did not experience high power degradation, which was an unexpected result. However, cells showed increased variability in degradation when cells were cycled at the same temperature [128]. One research [39] studied the lifetime of battery energy storage systems under various assumptions. However, the assumption of feasibility was missing due to the arbitrary choice of battery cell charge and recharge thresholds to trigger corrective measures. The role of battery management can improve the lifetime of batteries by selecting optimal charging strategies. The battery management improves the operation by limiting the unnecessary rate of charge to ensure optimal operation of the battery achieved [43], [47]. An investigation [129] presented a life prediction approach considering the battery's EoL criteria as a failure and tested these failures time data to evaluate reliability assessment of lithium secondary batteries. Another study [58] found that battery energy storage combined with dc-link and dc-to-dc converters may enhance the lifetime of batteries and provide a reliable and flexible design platform [58].

However, significant barriers to EV technology exist, such as the demand for the driving range and the demand for EV charging stations, thereby preventing the widespread use of EVs [124]. In our previous work [71], an empirical battery cycle aging model for V2G application, including daily driven patterns, was used to calculate annual battery wearing cost. A comparison of the considered methods with the contemporary literature regarding cycle life models and V2G operations shows the majority of the research covers only measurements and/or models (Table IV). Typical functions not considered are daily driven patterns, years or driving distance, and V2G operations.

All the considered methods: cycle life measurements, cycle aging models, daily driven patterns, battery life in years, calculated lifetime driving distance, and the V2G connection, were covered only in [55], [71]. The aging model examined the degradation of battery cells [55]. A number of charging times per day was included in the model to variate driving patterns.

TABLE IV
SALIENT FEATURES OF THE PROPOSED APPROACH IN COMPARISON WITH THE CONTEMPORARY CYCLE AGING STUDIES

Considered methods*	Measurements	Models	Daily driven patterns	Years or driving distance	V2G operations
[7]–[9], [22], [24], [29], [31]–[33], [42], [46], [47], [49], [52], [61], [65], [67]–[69]	X				
[125]		X			
[5], [6], [10], [12], [14]–[19], [21], [23], [26], [30], [35], [36], [39]–[41], [45], [48], [51], [52], [56], [57], [62], [63], [66]	X	X			
[25]	X		X		
[124]		X	X		
[50], [58], [59], [130], [131]	X	X	X		
[37], [59]	X			X	
[11], [20], [27], [60]	X	X		X	
[34]	X	X	X	X	
[43], [64], [70], [126]	X	X			X
[53]	X	X	X		X
[28]	X	X		X	X
[55], [71]	X	X	X	X	X

*For more detail, please refer to the cycle life studies references.

The aging model [71] examined the degradation of battery cells, including calendar and cycle aging. The novelty of the proposed study, in respect to the previous work published [71], is the development stage of charge limits, which include a number of chargings per day. This development provides an effective way to control SoC value, which is one of the main reasons for calendar aging. The loading behavior adapted various driving scenarios and charging schemes [55]. V2G operations can provide peak shaving service for the power grid [55]. The findings [55] demonstrated that V2G operations reduced the battery cell life due to the prolonged discharging and greater cycle depths in discharging. However, intelligent charging schemes may enhance battery life.

A great amount of literature [5], [6], [10], [12], [14]–[19], [21], [23], [26], [30], [35], [36], [39]–[41], [45], [48], [51], [52], [56], [57], [62], [63], [66] presented battery cycle measurements and battery aging models. Only a few studies [28], [55], [71] discussed battery lifetime in years, calculated lifetime driving distance and provided V2G operations. Therefore, grid operators could perform V2G operations in the future through different aggregation schemes, which involve an agent and multi-agent logic. For this reason, grid operators will probably avoid direct real-time control in the future.

The proposed investigation procedure shown in Fig. 1 intends to first calculate the average driving distance from initial values of an EV and batteries and from driving data. The second step involves four charge limits leading to four distances for the charging range to calculate equivalent full cycles. The third stage measurement data shows the cycle

This article has been accepted for publication in a future issue of this journal, but has not been fully edited. Content may change prior to final publication. Citation information: DOI 10.1109/JESTPE.2019.2959276, IEEE Journal of Emerging and Selected Topics in Power Electronics

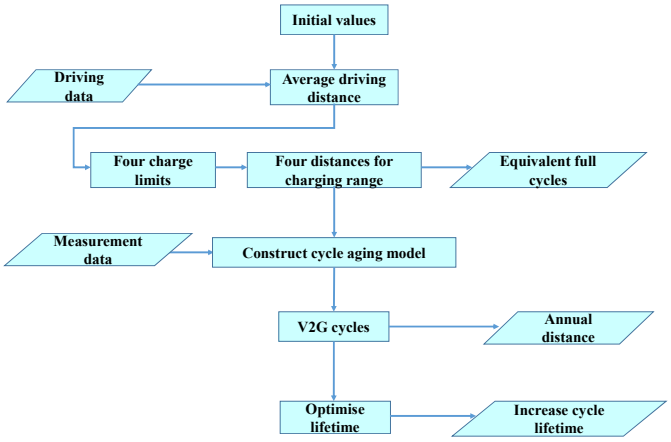

Fig. 1. The proposed investigation procedure. Inputs are driving data and measurement data. Outputs are equivalent full cycles, annual distance and increase cycle lifetime.

life of the batteries, where measurements are validated by comparing to other measurement data [23]. A number of V2G cycles are randomly chosen and the corresponding annual distance is calculated. Cycle lifetime is optimized to enhance the cycle life for battery cells.

VI. Configuration for the Battery Model

The main reasons for Li-ion degradations are i) Li-ion deposition, ii) passive film growth, iii) crack propagation and iv) an active lithium anodic dissolution [75]. The main reason for calendar aging is Li-ion deposition and for cycle aging, Li-ion plating. Time, temperature and SoC are the main reasons for calendar aging of the battery cell. The main reasons for cycle aging are DoD, charge/discharge rate and temperature [75]. This battery model does to consider reasons for aging separately, only cycle lifetime in years.

A. Annual equivalent full cycles

Battery lifetime equations [71] are implemented for the battery cell cycle aging model and initial values such as range and battery capacity are collected. Information about daily driven distances [73] of 179,484 cars showed that on a daily basis 19%, 21%, and 16% of the drivers would travel 8 km, 24 km, and 40 km, respectively, whereas in total, 85% would travel up to 105 km (Fig. 2); this is used as the base data for the proposed calculations. The proposed methodology divides the battery charging into four charge limits according to travel distances. Battery lifetime is optimized by choosing the optimal charge limit.

Full cycle means that the full EV range is used. When batteries are charged and discharged partly, only a fraction of the battery capacity is used. Partly charged distance is compared to the range, called the equivalent full cycle. Equations are implemented for the battery cell cycle aging model to calculate the lifetime and the cost of V2G operations. The battery cell temperature used in the calculation is 35 °C, charging rate

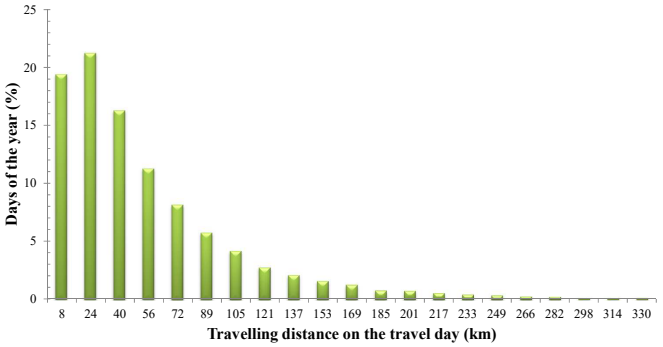

Fig. 2. Daily traveling distances. The distribution of the total driving distance on the travel day.

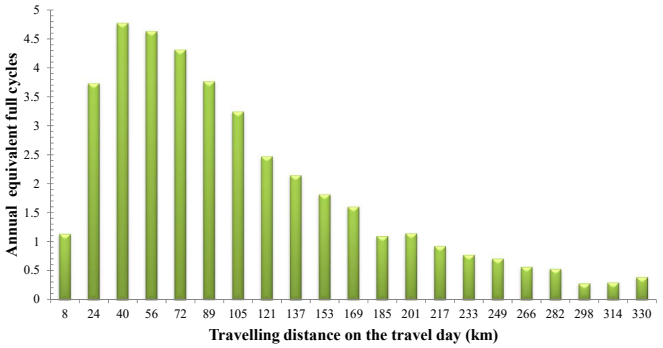

Fig. 3. Annual equivalent full cycles divided into annual traveling categories.

1 It, and SoCs are 5%, 10%, 15%, and 20%. Equation (1) calculates equivalent full cycles a year

$$N_{acd} = \frac{D_{dd}}{D_{range}} \cdot N_d \,, \tag{1}$$

where D_{dd} is the daily distance drove, D_{range} is the driving range and N_d is the number of annual driving days.

Equation (1) offers an equivalent full cycle, which means that a traveling distance is equivalent full cycle times a range. In this case, the shortest charge limit (SoC 5%) is sufficient to cover driving and only one charging is needed that specific day.

Fig. 3 shows the equivalent full cycles per traveling distance calculated from (1). The physical implication of (1) is the degradation of batteries, because of traveling distance. Compared to Fig. 2, degradation is relatively higher at longer distances because the annual distance is higher.

The annual driving distance can be calculated as

$$D_{ad} = \Sigma(N_d \cdot D_{dd}) \,. \tag{2}$$

Values for calculating the annual driving distance (2) is derived from driving data.

VII. Battery Cell Aging Tests

In battery cell aging tests, charging and discharging cycles were around a mean of 50% SoC [11]. A mean of 50% SoC is determined as optimal for enhancing battery cell life [11]. Fig. 4 shows that the lowest battery cell cycle depth provides

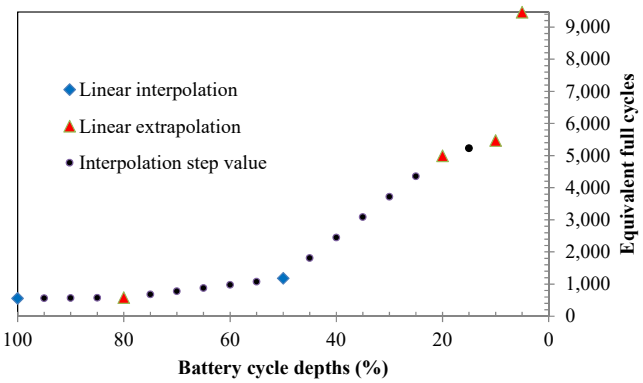

Fig. 4. Measured battery cycle depths when the average value is 50% SoC. Values are interpolation or extrapolation values from measurement data.

the longest lifetime, and the highest cycle depth provides the shortest life expectancy. The battery cell aging model focuses on extended lifetime parameters. V2G operations use the lowest cycle depth value of 5%, as it provides the highest number of equivalent full cycles. To enhance the EV battery cell lifetime, the battery cell aging model chooses four lowest cycle depths: 5%, 10%, 15%, and 20% as charge limits for driving.

The four highest equivalent full cycles in Fig. 4 are used for driving and the highest value for V2G operations. Cycle numbers 4,993; 5,470; 9,461 are calculated by using linear interpolation from measurement data [11] for SoC values 20%, 10%, and 5%. Missing cycle number value 5,231 for 15% SoC is calculated by using the interpolation step value.

A. Charge limits

Equivalent full cycles N_{cn} and used cycles N_{acm} are used for calculating battery cell lifetime aging N_l. Equivalent full cycles and used cycles are collected from the annual equivalent full cycles. Four charge limits are limiting distances. An EV range means the total range per charge. A range is where the maximum available driving distance and actual driving distance need to be smaller than range. For example, charge limit 1 could have the longest distance of 100 km and batteries will be charged every 100 km distance. With charge limit 1, we can obtain 4,993 equivalent full cycles.

B. Calculated aging for battery cells

Battery cell lifetime aging N_l can be calculated using

$$N_{acm} = \frac{\Sigma N_{acm}}{\Sigma \dfrac{N_{acm}}{N_{cn}}} . \tag{3}$$

where N_{acm} is annual equivalent full cycles and N_{cn} is equivalent full cycles.

Four charge limits number values after calculation (3), generate 5,484 cycles for a lifetime. The equivalent full cycle N_{cn} is calculated from the measured cycles. In other words, temperature, SoC and It-rate are included in this value. The physical implication of (3) is transforming lifetime cycles from battery measurements to lifetime driving distance with the help of vehicle range.

C. Lifetime compensation for V2G operations

The grid operator can choose a number of V2G cycles a day N_c according to the balance situation of the power grid. The equations adapt driving patterns. To enhance battery life, V2G operations' charging and discharging cycle is from 47.5% to 52.5% SoC. A number of V2G cycles a day N_c are transformed into annual equivalent full cycles N_{V2G} by calculating

$$N_{V2G} = \frac{N_c \cdot 5}{100} \cdot 365 , \tag{4}$$

where N_c is the chosen V2G cycles a day.

The cycle aging model variates V2G cycles between 16 and 32. Annual equivalent full cycles N_{V2G} for V2G operations are transformed to a driving distance D_{ae} by multiplying N_{V2G} by the driving range. If N_c is 24 V2G cycles, then the grid operator uses 24 V2G cycles from EV batteries. The nature of the V2G cycles is that battery management discharges batteries from 52.5% to 47.5% SoC and then recharges batteries up to 52.5% SoC. This is one V2G cycle. In this case, these cycles are repeated 24 times a day.

The calculated V2G fraction is the relation between V2G cycles and maximum available cycles N_{c4}

$$F_{V2G} = \frac{N_{V2G}}{N_{c4}} , \tag{5}$$

where N_{c4} is equivalent full cycles with a charge limit of 4.

Charge limit 4 is used for V2G regulation because it has the largest number of equivalent full cycles (9,461). The physical implication of (5) is to show how a large fraction of total battery energy is provided for the V2G regulation.

The fraction of battery cell charge F_{ad}, which is used for annual driving, is calculated from cell equivalent full cycles and used cycles

$$F_{ad} = \Sigma \frac{N_{acm}}{N_{cn}} . \tag{6}$$

where N_{acm} are cycles used for driving with four charge limits and N_{cn} is equivalent full cycles.

The physical implication of (6) is to show how a large fraction of total battery energy is used for driving.

V2G operations reduce driving distance. The driving distance reduction D_{ar} can be calculated as

$$D_{ar} = \frac{D_{ad}}{F_{ad}} \cdot F_{V2G} , \tag{7}$$

where D_{ad} is the EV driving distance a year (2), F_{ad} is the fraction of battery charge used for driving (6) and F_{V2G} is the fraction of V2G cycles.

The physical implication of (7) is to show how much a V2G operation degrades EV batteries.

After a V2G operation's reduction, we calculate battery life as a driving distance with an optimal charging schedule

$$D_{ld} = \frac{D_{ad}}{F_{ad} + F_{V2G}} . \tag{8}$$

The obtained driving distance articulates the longest driving distance before batteries need to change. Battery cells have reduced driving distance with V2G usage.

Cycle life of the EV batteries T_l can be calculated as

$$T_l = \frac{D_{ld}}{D_{ad}}\,. \tag{9}$$

In this equation (9), lifetime value T_l suggests cycle life, not the calendar life of the EV batteries. These lifetimes are ideal cycle lifetimes with optimized charging patterns and V2G cycles. Calendar life is giving a limit to the lifetime, which is not included in this equation.

The distance reduction is based on charging-discharging cycles used in V2G operations, which reduce battery lifetime. The distance reduction during the lifetime D_{lr} explains how much V2G operations consume battery life,

$$D_{lr} = D_l - D_{ld}\,, \tag{10}$$

where D_l is maximum driving distance during a lifetime without V2G operations and D_{ld} is driving distance during a lifetime with V2G operations (8).

The grid operator receives benefits from V2G operations and needs to compensate for battery degradation due to V2G operations to the EV battery owner. V2G compensation during the lifetime P_{lc} can be calculated as

$$P_{lc} = \frac{D_{lr}}{D_l} \cdot P_b\,, \tag{11}$$

where P_b is the purchase cost of an EV battery pack.

We can calculate the annual compensation of battery wear P_{ac} for V2G operations using the equation

$$P_{ac} = \frac{D_{ar}}{D_l} \cdot P_b\,. \tag{12}$$

As a result, annual V2G compensation P_{ac} for battery cells is calculated, from which grid operators compensate because of battery wear. For that investment, grid operators receive V2G cycles to support power grid balance. If the number of V2G cycles N_c is lower, the annual grid operators compensation is lower. Therefore, if numbers of V2G cycles are increased, grid operators need to compensate more for the V2G operations. As a result, from the grid operators point of view, battery cells are attractive for V2G operations.

The annual energy E_{V2G} transferred because of V2G operations can be calculated as

$$E_{V2G} = \frac{E_b \cdot 5}{100} \cdot N_c \cdot 365\,, \tag{13}$$

where E_b is EV battery capacity.

Annual energy E_{V2G} for battery cells is calculated from equation (13). This energy is cycled between the battery and power grid. Electricity price P_{kWh}, which is used for V2G operations is calculated

$$P_{kWh} = \frac{P_{ac}}{E_{V2G}}\,. \tag{14}$$

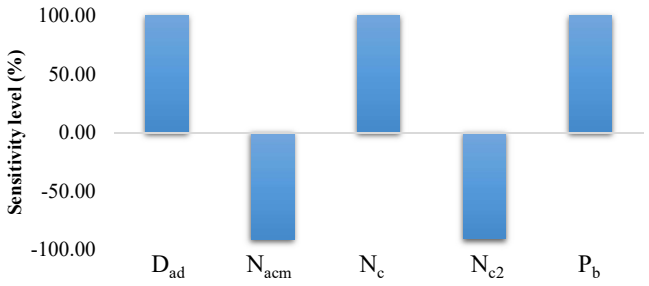

Fig. 5. Sensitivity levels for annual distance drove (D_{ad}), equivalent full cycles a year (N_{acm}), number of V2G cycles (N_c), and equivalent full cycles in V2G charge limit (N_{cn}) and battery package cost (P_b).

Electricity price P_{kWh} for battery cells is calculated. Power grid uses the V2G operation for frequency regulation. Electricity flows from batteries to the power grid when the power grid frequency is low. When the power grid frequency is high, electricity flows from the power grid to batteries. This means that the grid operator needs to pay a relatively low energy price for the use of battery cells. From the grid operators point of view, battery cells are attractive for V2G operations.

Annual V2G compensation P_{ac} (12) is combined from equations (2), (4), (6) and (7).

$$P_{ac} = \frac{\Sigma_{n=1}^{19}(N_d \cdot D_{dd})_n \cdot N_c \cdot 5 \cdot 365 \cdot P_b}{100 \cdot N_{cn} \cdot \Sigma_{n=1}^{4}(N_{acm})_n \cdot D_{range}}\,. \tag{15}$$

The sensitivity test determines the relative significance of the input variables. The sensitivity of variables in (15) is calculated by multiplying each variable by 10. The change in output (P_{ac}) is compared to the input variable. The method proposed by [132], [133] is utilized.

$$S = \frac{\Delta Output}{\Delta Input} \cdot 100\,. \tag{16}$$

D_{ad}	D_{range}	N_{acm}	N_c	N_{cn}	P_b
100.03	0	-90.93	100.03	-90.86	99.95

Fig. 5 shows sensitivity levels. Columns are nearly the same size. Positive columns increase annual V2G compensation and negative columns decrease annual V2G compensation. Annual distance driven (D_{ad}), number of V2G cycles (N_c) and battery package cost (P_b) increase annual V2G operations. Equivalent full cycles per year (N_{acm}) and V2G charge limit (N_{c4}) decrease annual V2G compensation. Range (D_{range}) does not affect annual V2G compensation.

VIII. Validation of Battery Aging Model

Battery aging tests are carried out for battery cells [11]. Battery cell tests carry charging and discharging cycles at the mean value of 50% SoC. Fig. 6 shows cell measurements with several SoCs [11]. Cycles between 0 and 100% SoC provide the shortest lifetime, and cycles between 47.5% and 52.5% SoC provide the longest life expectancy. The battery model

This article has been accepted for publication in a future issue of this journal, but has not been fully edited. Content may change prior to final publication. Citation information: DOI 10.1109/JESTPE.2019.2959276, IEEE Journal of Emerging and Selected Topics in Power Electronics

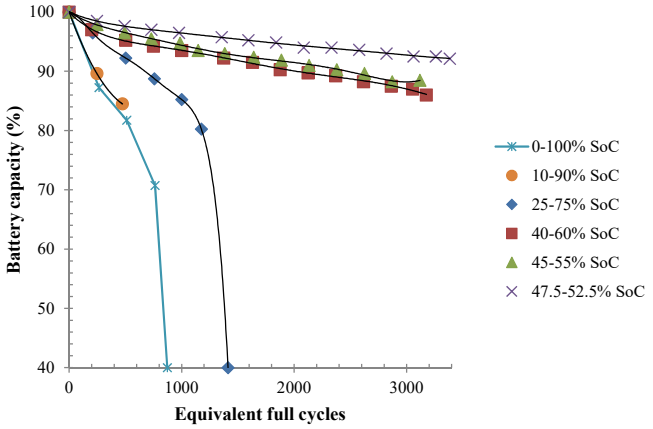

Fig. 6. Measurement results for battery capacity against equivalent full cycles. The study compares measured battery cycle depths around a mean of 50% SoC.

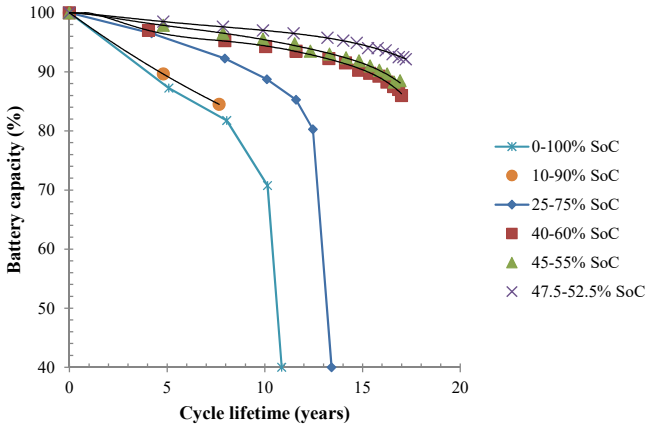

Fig. 7. Battery aging model results for battery capacity against cycle lifetime. The study compares measured battery cell discharging around a mean of 50% State of Charge (SoC).

selects optimal cycle areas to enhance the EV battery cell lifetime. Therefore, the battery model used 5%, 10%, 15%, and 20% cycle depths as charge limits.

Validation checks the accuracy of the battery cycle aging model. Battery measurements in Fig. 6 are a representation of the real system. Capacity fade is shown around an average SoC of 50%. The shortest lifetime expectation is cells cycled between 0 and 100%, the longest life is the cells cycled between 47.5% and 52.5% SoC.

We include similar charging-discharging windows in the battery aging model, Fig. 7. Instead of equivalent full cycles, cycle lifetime is calculated in years. The battery aging model is validated by measurement data from the database. There is a clear similarity between measurements and battery aging model results and capacity fade is predicted with acceptable accuracy. During the first years, batteries run a low number of cycles and in later years, batteries need more cycles because of battery degradation. This is why data points are more frequent at the end of the curves in Fig. 7.

The longest lifetime distance D_{ld} for battery cells and the lifetime value T_l for battery cells are calculated. The annual V2G compensation P_{ac} for battery cells with V2G

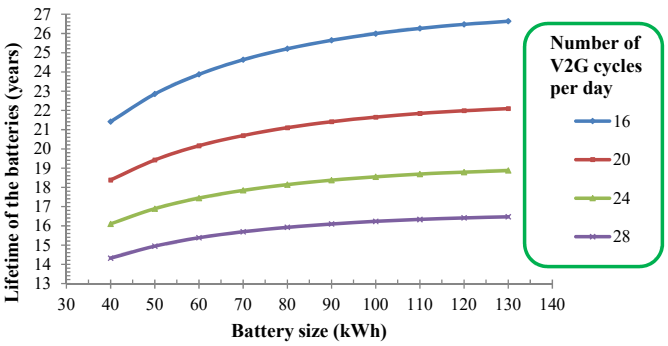

Fig. 8. A lifetime of the batteries with different Vehicle to Grid (V2G) cycles.

cycles and the energy E_{V2G} for battery cells are calculated. V2G operations transfer electricity between the grid and EV batteries. V2G operations' energy price P_{kWh} for battery cells is calculated [71].

Battery technologies are compared in terms of their durability when used in V2G operations. The battery cells' average charge is 50%. For example, for battery cells, 5% cycle depth is cycled between 47.5% and 52.5% SoC. For batteries, the lowest cycling depth provides the longest lifetime. For batteries, lifetime clearly increases when cycling depth is under 50%. The longest lifetime, 9,461 equivalent full cycles, is reached when cycling depth is 5%. When the range is 500 km, 5% means charging every 25 km. These low cycling depth values are possible if a battery pack is large enough. Using 5% of the battery cell capacity, the lifetime can be increased. The increased lifetime can be achieved if charging is done every 25 km, or more frequently, and the range needs to be large. If the range is small, charging requires high DoDs. This is why battery cells are suitable for EV with large battery capacity EV application. Controlled and uncontrolled charging brings different life expectancies for cells. This restricts V2G operation when a large amount of electric power needs to transferred to the power grid. Controlled and uncontrolled charging brings an obvious difference to EV battery cells. The SoC window should be strictly limited near 50% SoC, limiting the amount of transferred power. To elucidate findings, battery cells do not wear out in V2G operations, because available equivalent full cycles are 9,461.

In the V2G application, battery cells should have high equivalent full cycles. Battery cells have the highest equivalent full cycles when cells are cycled between 47.5% and 52.5% SoC [11]. To develop batteries for the V2G application, equivalent full cycles should be higher. Evaluation of battery life in the V2G application should be focused on improving the cell performances in the equivalent full cycle area.

The number of V2G cycles affects the lifetime of the EV battery. Battery lifetime curves are shown in Fig. 8. A number of V2G cycles and battery size affect the battery lifetime. The lowest number of V2G cycles provides the longest cycle life.

The lifetime for battery cells shown in Fig. 9. Lifetimes are long enough for EV use. The strongest signal of battery capacity fade is the processed battery energy, not DoD [53]. The contour plot shows that battery size is not an important

This article has been accepted for publication in a future issue of this journal, but has not been fully edited. Content may change prior to final publication. Citation information: DOI 10.1109/JESTPE.2019.2959276, IEEE Journal of Emerging and Selected Topics in Power Electronics

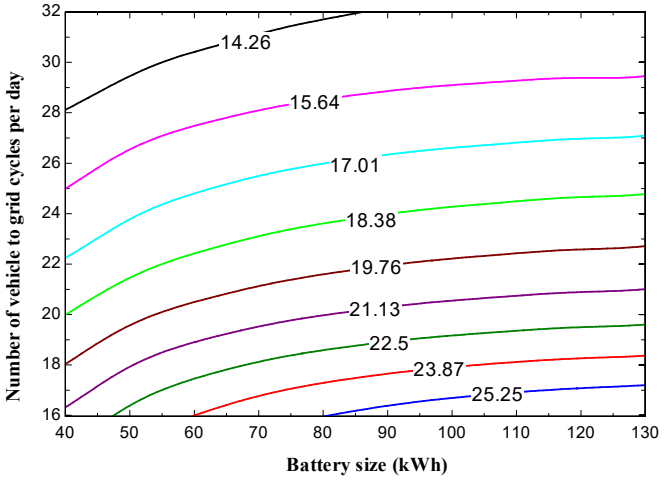

Fig. 9. Lifetime of the batteries in years. The contour plot for battery cells with Vehicle to Grid (V2G) operations.

factor; however, the number of V2G cycles degrade battery lifetime noticeably. From this contour plot, we can choose the desired battery cell cycle life and read corresponding battery size and number of V2G cycles. In calculations, battery size, number of V2G cycles and lifetime are variables in the parametric table. Equation (9) is used to plot Fig. 9. By increasing battery size, lifetime is increased and by increasing V2G cycles a day, lifetime is decreased.

IX. Interpretation and Discussion

In V2G operations, electricity flows from the main grid into the EV batteries, charging batteries, and from the EV batteries into the power grid, discharging batteries. Using direct real-time control of the grid operator, battery charger charges batteries provide V2G balance and frequency regulation to the grid. As smart charging is an important part of EV penetration, V2G may provide an important extension for smart charging procedures. To satisfying the scheduled charging, we propose to switch the V2G control to a smart charging control. EV batteries can be utilized as a flexible distributed energy resource [134]. The V2G concept is a development for the smart charging system allowing EVs to inject electricity into the distribution network. V2G operations utilize EVs as distributed generators and battery storage systems.

One of the merits of this review is that it provides some useful information for V2G battery selection. V2G reduces the lifetime of the batteries. Degradation is reduced by choosing an optimal charging window SoC. In batteries, 47.5% to 52.5% SoC shows prolonged lifetime thus EV batteries are suitable for V2G operations. One V2G cycle is 47.5% to 52.5% SoC and covers 5% window of battery capacity. Such a V2G cycle does not affect lifetime much. However, for V2G systems, smaller charging and discharging depths mean less flexibility in using battery energy for V2G operations. The global optimality of the V2G system could be severely biased. The battery model uses V2G cycles; every cycle is a 5% slide from the battery capacity. We did not study smaller discharge range in the manuscript, however, 1% capacity usage around 50% SoC may provide smaller effect on battery cycle life. Battery life consists of calendar life as well as cycle life. Calculated cycle life means numbers of cycles. If calendar life is lower than cycle life, the user can increase V2G cycles to receive more income. The total life is either calendar life or cycle life, which comes earlier.

Low charge level is avoided because usually empty batteries are thought to have accelerated aging. However, EV battery measurements show that prolonged calendar life is received with empty batteries. This seems to be in conflict with cycle life measurements. Battery cell degradation behavior is different in the calendar life test from cycle life test. Most of cell aging models validate results with measurements and capacity fade is predicted with acceptable accuracy.

Vehicle information is from battery EV. The range and battery capacity is recorded. These choices construct a connection to real-life as these batteries are used in EV configuration. Usually, lifetime prediction shows a prolonged lifetime in the 47.5% to 52.5% SoC area. The cycling experiments with $Li(NiMnCo)O_2$ battery cells indicated that cycling around a mean value of 50% provides the longest battery cell lifetime. It is not clear whether this recommendation applies to all the battery chemistries studied.

Except for the V2G operations' impact study, the key and significant findings in the review of the literature indicated that calendar aging is particularly influenced by stationary time, SoC, and temperature, while cycle aging is particularly influenced by a number of charges and discharges, DoD, and rate of charge. Chemical reasons in the aging processes are lithium deposition, the formation of passive films, crack propagation, as well as an active lithium dissolution in the electrode.

X. Conclusion

This paper reviewed cycle aging studies. In published works, Li-ion batteries dominate electric vehicle battery applications. A review of cycle aging tests and cycle aging models was presented. Time, temperature as well as the state of charge influence calendar aging. A number of charging cycles in vehicle to grid operations, depth of discharge as well as the rate of charging influence cycle aging. The focus in reviewed papers was aging measurements and models. Many factors for degradation were revived. However, solutions to enhance battery life are not well understood. Hence, the cycle aging model was proposed and charge limits were used to enhance battery life. Research papers were organized by cycle aging measurements and methods for cycle aging studies were considered. Principal findings are that lifetime reduction is decreased in vehicle to grid operations and a lifetime can be extended. Optimal charge levels are used in vehicle to grid operations and selected charge levels are used in driving. This study is important to the community and is noteworthy because it shows an extended lifetime with battery management instead of developing battery chemistry. Implications of the findings are the importance of a battery management system in vehicle to grid operations, and vehicle to grid operations will become a more compelling technology. The review, as well as the

findings, address the defined objective by decreasing lifetime influence from vehicle to grid operations. Battery cell wearing is studied for battery cells. The author concludes that battery cells are suitable for an electric vehicle with a large battery capacity electric vehicle application. With large battery capacity, only a small fraction of battery capacity is used for driving. With small battery capacity, a full charge and discharge are frequently needed. The difference between large cells' and small cells' lifetimes is significant. Lifetime is calculated for battery cells. Vehicle to grid operations provide frequency regulation for the power grid. Energy used for vehicle to grid operations and energy price is calculated for battery cells. Power grid operators compensate energy used for vehicle to grid operations. If the battery charge is kept around 50%, battery cells' lifetime can be enhanced. Investigated cells can be simulated with different variables and cycle life optimized.

NOMENCLATURE

AC	Alternating current
D_{ad}	Annual driving distance
D_{ae}	Annual equivalent V2G distance
D_{ar}	Annual V2G distance reduction
D_{dd}	Daily distance drove
D_l	Lifetime driving distance
D_{ld}	Lifetime driving distance with the V2G operations
D_{lr}	Driving distance consumed by V2G operations
DoD	Depth of Discharge
D_{range}	Maximum driving distance per one charge
E_b	Battery energy capacity
EoL	End of Life
EV	Electric Vehicle
E_{V2G}	Annual energy used for V2G
F_{ad}	The fraction of battery capacity used for driving
F_{V2G}	The fraction of V2G cycles to the maximum number of cycles
It	Discharge current rate related to capacity
LCO	Lithium Cobalt Oxide $LiCoO_2$
LCP	Lithium Cobalt Phosphate $LiCoPO_4$
LFP	Lithium Iron Phosphate $LiFePO_4$
LFSF	Lithium Iron Fluoro Sulphate $LiFeSO_4F$
Li-ion	Lithium-ion
LMO	Lithium Manganese Oxide $LiMnO_2$ $Li_2Mn_2O_4$
LMP	Lithium Manganese Phosphate $LiMnPO_4$
LNO	Lithium Nickel Oxide $LiNiO_2$
LTO	Lithium Titanium Oxide Li_2TiO_3
LTS	Lithium Titanium Sulphide $LiTiS_2$
LVP	Lithium Vanadium Phosphate $Li_3V_2(PO_4)_3$
MFCP	Lithium Manganese Iron Cobalt Phosphate $LiMn_{1/3}Fe_{1/3}Co_{1/3}PO_4$
N_{acd}	Equivalent full cycles a year
N_{acm}	Used cycles, all charge limits
N_c	Number of cycles for V2G operations
N_{c4}	Equivalent full cycles, charge limit four
NCA	Lithium Nickel Cobalt Aluminium oxide $LiNiCoAlO_2$
NCM	Lithium Nickel Cobalt Manganese oxide $LiNi_xCo_yMn_zO_2$
N_{cn}	Lifetime equivalent full cycles
NCP	Lithium Nickel Cobalt Phosphate $LiNi_{0.5}Co_{0.5}PO_4$
N_d	Number of days
N_l	Battery lifetime wearing
NMC	Lithium Nickel Cobalt Manganese oxide $LiNi_xCo_yMn_zO_2$
NMO	Lithium Nickel Manganese Oxide $Li(Ni_{0.5}Mn_{0.5})O_2$
N_{V2G}	Annual equivalent full V2G cycles
P_{ac}	Annual V2G compensation
P_b	Estimated battery package cost
P_{kWh}	Energy price used for V2G
P_{lc}	Lifetime compensation for V2G usage
RPT	Reference Performance Test
SEI	Solid Electrolyte Interface
SoC	State of Charge
SoH	State of Health
T_l	A lifetime of the batteries
V2G	Vehicle to Grid

REFERENCES

[1] K. Rajashekara, "Present status and future trends in electric vehicle propulsion technologies," *IEEE Journal of Emerging and Selected Topics in Power Electronics*, vol. 1, no. 1, pp. 3–10, 2013.

[2] Z. Asus, E.-H. Aglzim, D. Chrenko, Z.-H. C. Daud, and L. Le Moyne, "Dynamic modeling and driving cycle prediction for a racing series hybrid car," *IEEE Journal of Emerging and Selected Topics in Power Electronics*, vol. 2, no. 3, pp. 541–551, 2014.

[3] D. M. Hill, A. S. Agarwal, and F. Ayello, "Fleet operator risks for using fleets for V2G regulation," *Energy Policy*, vol. 41, pp. 221–231, 2012, modeling Transport (Energy) Demand and Policies.

[4] F. Tedesco, L. Mariam, M. Basu, A. Casavola, and M. F. Conlon, "Economic model predictive control-based strategies for cost-effective supervision of community microgrids considering battery lifetime," *IEEE Journal of emerging and selected topics in power electronics*, vol. 3, no. 4, pp. 1067–1077, 2015.

[5] A. Eddahech, O. Briat, H. Henry, J. Y. Delétage, E. Woirgard, and J. M. Vinassa, "Ageing monitoring of lithium-ion cell during power cycling tests," *Microelectronics Reliability*, vol. 51, no. 9-11, pp. 1968–1971, 2011.

[6] T. G. Zavalis, M. Klett, M. H. Kjell, M. Behm, R. W. Lindström, and G. Lindbergh, "Aging in lithium-ion batteries: model and experimental investigation of harvested LiFePO4 and mesocarbon microbead graphite electrodes," *Electrochimica Acta*, vol. 110, pp. 335–348, 2013.

[7] P. Liu, J. Wang, J. Hicks-Garner, E. Sherman, S. Soukiazian, M. Verbrugge, H. Tataria, J. Musser, and P. Finamore, "Aging mechanisms of LiFePO4 batteries deduced by electrochemical and structural analyses," *Journal of the Electrochemical Society*, vol. 157, no. 4, pp. A499–A507, 2010.

[8] M. Safari and C. Delacourt, "Aging of a commercial graphite/LiFePO4 cell," *Journal of The Electrochemical Society*, vol. 158, no. 10, pp. A1123–A1135, 2011.

[9] S. Barcellona, M. Brenna, F. Foiadelli, M. Longo, and L. Piegari, "Analysis of ageing effect on Li-polymer batteries," *The Scientific World Journal*, vol. 2015, 2015.

[10] E. Sarasketa-Zabala, I. Gandiaga, L. M. Rodriguez-Martinez, and I. Villarreal, "Calendar ageing analysis of a LiFePO4/graphite cell with dynamic model validations: towards realistic lifetime predictions," *Journal of Power Sources*, vol. 272, pp. 45–57, 2014.

[11] M. Ecker, N. Nieto, S. Käbitz, J. Schmalstieg, H. Blanke, A. Warnecke, and D. U. Sauer, "Calendar and cycle life study of Li (NiMnCo) O2-based 18650 lithium-ion batteries," *Journal of Power Sources*, vol. 248, pp. 839–851, 2014.

[12] J. Belt, V. Utgikar, and I. Bloom, "Calendar and PHEV cycle life aging of high-energy, lithium-ion cells containing blended spinel and layered-oxide cathodes," *Journal of Power Sources*, vol. 196, no. 23, pp. 10 213–10 221, 2011.

[13] G. Ning, B. Haran, and B. N. Popov, "Capacity fade study of lithium-ion batteries cycled at high discharge rates," *Journal of power sources*, vol. 117, no. 1-2, pp. 160–169, 2003.

[14] X. Li, J. Jiang, L. Y. Wang, D. Chen, Y. Zhang, and C. Zhang, "A capacity model based on charging process for state of health estimation of lithium ion batteries," *Applied energy*, vol. 177, pp. 537–543, 2016.

[15] M. Dubarry, C. Truchot, and B. Y. Liaw, "Cell degradation in commercial LiFePO4 cells with high-power and high-energy designs," *Journal of Power Sources*, vol. 258, pp. 408–419, 2014.

[16] X. Han, M. Ouyang, L. Lu, J. Li, Y. Zheng, and Z. Li, "A comparative study of commercial lithium ion battery cycle life in electrical vehicle: aging mechanism identification," *Journal of Power Sources*, vol. 251, pp. 38–54, 2014.

[17] V. Muenzel, A. F. Hollenkamp, A. I. Bhatt, J. de Hoog, M. Brazil, D. A. Thomas, and I. Mareels, "A comparative testing study of commercial 18650-format lithium-ion battery cells," *Journal of The Electrochemical Society*, vol. 162, no. 8, pp. A1592–A1600, 2015.

[18] E. Sarasketa-Zabala, I. Gandiaga, E. Martinez-Laserna, L. M. Rodriguez-Martinez, and I. Villarreal, "Cycle ageing analysis of a LiFePO4/graphite cell with dynamic model validations: towards realistic lifetime predictions," *Journal of Power Sources*, vol. 275, pp. 573–587, 2015.

[19] K. Jalkanen, J. Karppinen, L. Skogström, T. Laurila, M. Nisula, and K. Vuorilehto, "Cycle aging of commercial NMC/graphite pouch cells at different temperatures," *Applied Energy*, vol. 154, pp. 160–172, 2015.

[20] S. Käbitz, J. B. Gerschler, M. Ecker, Y. Yurdagel, B. Emmermacher, D. André, T. Mitsch, and D. U. Sauer, "Cycle and calendar life study of a graphite— LiNi1/3Mn1/3Co1/3O2 Li-ion high energy system. Part A: full cell characterization," *Journal of Power Sources*, vol. 239, pp. 572–583, 2013.

[21] Y.-J. Lee, H.-Y. Choi, C.-W. Ha, J.-H. Yu, M.-J. Hwang, C.-H. Doh, and J.-H. Choi, "Cycle life modeling and the capacity fading mechanisms in a graphite/LiNi 0.6 Co 0.2 Mn 0.2 O 2 cell," *Journal of Applied Electrochemistry*, vol. 45, no. 5, pp. 419–426, 2015.

[22] X.-Y. Zhou, Y.-L. Zou, G.-J. Zhao, and J. Yang, "Cycle life prediction and match detection in retired electric vehicle batteries," *Transactions of Nonferrous Metals Society of China*, vol. 23, no. 10, pp. 3040–3045, 2013.

[23] J. Wang, P. Liu, J. Hicks-Garner, E. Sherman, S. Soukiazian, M. Verbrugge, H. Tataria, J. Musser, and P. Finamore, "Cycle-life model for graphite-LiFePO4 cells," *Journal of Power Sources*, vol. 196, no. 8, pp. 3942–3948, 2011.

[24] M. M. Joglekar and N. Ramakrishnan, "Cyclic capacity fade plots for aging studies of Li-ion cells," *Journal of Power Sources*, vol. 230, pp. 143–147, 2013.

[25] Y. Zhang, C.-Y. Wang, and X. Tang, "Cycling degradation of an automotive LiFePO4 lithium-ion battery," *Journal of Power Sources*, vol. 196, no. 3, pp. 1513–1520, 2011.

[26] D.-I. Stroe, M. Swierczynski, A.-I. Stroe, R. Laerke, P. C. Kjaer, and R. Teodorescu, "Degradation behavior of lithium-ion batteries based on lifetime models and field measured frequency regulation mission profile," *IEEE Transactions on Industry Applications*, vol. 52, no. 6, pp. 5009–5018, 2016.

[27] M. Ecker, J. B. Gerschler, J. Vogel, S. Käbitz, F. Hust, P. Dechent, and D. U. Sauer, "Development of a lifetime prediction model for lithium-ion batteries based on extended accelerated aging test data," *Journal of Power Sources*, vol. 215, pp. 248–257, 2012.

[28] M. Petit, E. Prada, and V. Sauvant-Moynot, "Development of an empirical aging model for Li-ion batteries and application to assess the impact of vehicle-to-grid strategies on battery lifetime," *Applied energy*, vol. 172, pp. 398–407, 2016.

[29] I. Bloom, L. K. Walker, J. K. Basco, D. P. Abraham, J. P. Christophersen, and C. D. Ho, "Differential voltage analyses of high-power lithium-ion cells. 4. Cells containing NMC," *Journal of Power Sources*, vol. 195, no. 3, pp. 877–882, 2010.

[30] D. Yan, L. Lu, Z. Li, X. Feng, M. Ouyang, and F. Jiang, "Durability comparison of four different types of high-power batteries in HEV and their degradation mechanism analysis," *Applied energy*, vol. 179, pp. 1123–1130, 2016.

[31] T. Guan, S. Sun, Y. Gao, C. Du, P. Zuo, Y. Cui, L. Zhang, and G. Yin, "The effect of elevated temperature on the accelerated aging of LiCoO2/mesocarbon microbeads batteries," *Applied energy*, vol. 177, pp. 1–10, 2016.

[32] B. Stiaszny, J. C. Ziegler, E. E. Krauß, J. P. Schmidt, and E. Ivers-Tiffée, "Electrochemical characterization and post-mortem analysis of aged LiMn2O4–Li (Ni0. 5Mn0. 3Co0. 2) O2/graphite lithium ion batteries. Part I: cycle aging," *Journal of Power Sources*, vol. 251, pp. 439–450, 2014.

[33] M. Dubarry, C. Truchot, B. Y. Liaw, K. Gering, S. Sazhin, D. Jamison, and C. Michelbacher, "Evaluation of commercial lithium-ion cells based on composite positive electrode for plug-in hybrid electric vehicle applications. Part II. Degradation mechanism under 2C cycle aging," *Journal of Power Sources*, vol. 196, no. 23, pp. 10 336–10 343, 2011.

[34] P. Gyan, P. Aubret, J. Hafsaoui, F. Sellier, S. Bourlot, S. Zinola, and F. Badin, "Experimental assessment of battery cycle life within the SIMSTOCK research program," *Oil & Gas Science and Technology–Revue dIFP Energies nouvelles*, vol. 68, no. 1, pp. 137–147, 2013.

[35] W. Waag, S. Käbitz, and D. U. Sauer, "Experimental investigation of the lithium-ion battery impedance characteristic at various conditions and aging states and its influence on the application," *Applied energy*, vol. 102, pp. 885–897, 2013.

[36] F. Todeschini, S. Onori, and G. Rizzoni, "An experimentally validated capacity degradation model for Li-ion batteries in PHEVs applications," *IFAC Proceedings Volumes*, vol. 45, no. 20, pp. 456–461, 2012.

[37] D. Anseán, M. González, J. C. Viera, V. M. García, C. Blanco, and M. Valledor, "Fast charging technique for high power lithium iron phosphate batteries: a cycle life analysis," *Journal of Power Sources*, vol. 239, pp. 9–15, 2013.

[38] C. Dudézert, Y. Reynier, J.-M. Duffault, and S. Franger, "Fatigue damage approach applied to Li-ion batteries ageing characterization," *Materials Science and Engineering: B*, vol. 213, pp. 177–189, 2016.

[39] A. Zeh, M. Müller, M. Naumann, H. Hesse, A. Jossen, and R. Witzmann, "Fundamentals of using battery energy storage systems to provide primary control reserves in Germany," *Batteries*, vol. 2, no. 3, p. 29, 2016.

[40] C. Meis, S. Mueller, S. Rohr, M. Kerler, and M. Lienkamp, "Guide for the focused utilization of aging models for Lithium-ion batteries-an automotive perspective," *SAE International Journal of Passenger Cars-Electronic and Electrical Systems*, vol. 8, no. 2015-01-0255, pp. 195–206, 2015.

[41] J. Schmalstieg, S. Käbitz, M. Ecker, and D. U. Sauer, "A holistic aging model for Li (NiMnCo) O2 based 18650 lithium-ion batteries," *Journal of Power Sources*, vol. 257, pp. 325–334, 2014.

[42] M. Dubarry, B. Y. Liaw, M.-S. Chen, S.-S. Chyan, K.-C. Han, W.-T. Sie, and S.-H. Wu, "Identifying battery aging mechanisms in large format Li ion cells," *Journal of Power Sources*, vol. 196, no. 7, pp. 3420–3425, 2011.

[43] B. Lunz, Z. Yan, J. B. Gerschler, and D. U. Sauer, "Influence of plug-in hybrid electric vehicle charging strategies on charging and battery degradation costs," *Energy Policy*, vol. 46, pp. 511–519, 2012.

[44] A. Marongiu, M. Roscher, and D. U. Sauer, "Influence of the vehicle-to-grid strategy on the aging behavior of lithium battery electric vehicles," *Applied Energy*, vol. 137, pp. 899–912, 2015.

[45] C. Ozkurt, F. Camci, V. Atamuradov, and C. Odorry, "Integration of sampling based battery state of health estimation method in electric vehicles," *Applied energy*, vol. 175, pp. 356–367, 2016.

[46] M. Fleischhammer, T. Waldmann, G. Bisle, B.-I. Hogg, and M. Wohlfahrt-Mehrens, "Interaction of cyclic ageing at high-rate and low temperatures and safety in lithium-ion batteries," *Journal of Power Sources*, vol. 274, pp. 432–439, 2015.

[47] S. Bourlot, P. Blanchard, and S. Robert, "Investigation of aging mechanisms of high power Li-ion cells used for hybrid electric vehicles," *Journal of Power Sources*, vol. 196, no. 16, pp. 6841–6846, 2011.

[48] C. Delacourt and M. Safari, "Life simulation of a graphite/LiFePO4 cell under cycling and storage," *Journal of The Electrochemical Society*, vol. 159, no. 8, pp. A1283–A1291, 2012.

[49] M. C. Smart, B. V. Ratnakumar, L. D. Whitcanack, F. J. Puglia, S. Santee, and R. Gitzendanner, "Life verification of large capacity Yardney Li-ion cells and batteries in support of NASA missions," *International Journal of Energy Research*, vol. 34, no. 2, pp. 116–132, 2010.

[50] M. Swierczynski, D.-I. Stroe, A.-I. Stan, R. Teodorescu, and S. K. Kær, "Lifetime estimation of the anophosphateLiFePO$_4$/C battery chemistry used in fully electric vehicles," *IEEE Transactions on industry Applications*, vol. 51, no. 4, pp. 3453–3461, 2015.

[51] I. Baghdadi, O. Briat, J.-Y. Delétage, P. Gyan, and J.-M. Vinassa, "Lithium battery aging model based on Dakins degradation approach," *Journal of Power Sources*, vol. 325, pp. 273–285, 2016.

[52] N. Omar, M. A. Monem, Y. Firouz, J. Salminen, J. Smekens, O. Hegazy, H. Gaulous, G. Mulder, P. Van den Bossche, T. Coosemans *et al.*, "Lithium iron phosphate based battery–assessment of the aging parameters and development of cycle life model," *Applied Energy*, vol. 113, pp. 1575–1585, 2014.

[53] S. B. Peterson, J. Apt, and J. F. Whitacre, "Lithium-ion battery cell degradation resulting from realistic vehicle and vehicle-to-grid utilization," *Journal of Power Sources*, vol. 195, no. 8, pp. 2385–2392, 2010.

[54] A. Friesen, C. Schultz, G. Brunklaus, U. Rodehorst, A. Wilken, J. Haetge, M. Winter, and F. Schappacher, "Long term aging of automotive type lithium-ion cells," *ECS Transactions*, vol. 69, no. 18, pp. 89–99, 2015.

[55] C. Guenther, B. Schott, W. Hennings, P. Waldowski, and M. A. Danzer, "Model-based investigation of electric vehicle battery aging by means of vehicle-to-grid scenario simulations," *Journal of Power Sources*, vol. 239, pp. 604–610, 2013.

[56] B. Xu, A. Oudalov, A. Ulbig, G. Andersson, and D. S. Kirschen, "Modeling of lithium-ion battery degradation for cell life assessment," *IEEE Transactions on Smart Grid*, vol. 9, no. 2, pp. 1131–1140, 2016.

[57] Z. Li, L. Lu, M. Ouyang, and Y. Xiao, "Modeling the capacity degradation of LiFePO4/graphite batteries based on stress coupling analysis," *Journal of Power Sources*, vol. 196, no. 22, pp. 9757–9766, 2011.

[58] S. Rothgang, T. Baumhöfer, H. van Hoek, T. Lange, R. W. De Doncker, and D. U. Sauer, "Modular battery design for reliable, flexible and multi-technology energy storage systems," *Applied Energy*, vol. 137, pp. 931–937, 2015.

[59] S. C. Nagpure, B. Bhushan, and S. S. Babu, "Multi-scale characterization studies of aged Li-ion large format cells for improved performance: an overview," *Journal of The Electrochemical Society*, vol. 160, no. 11, pp. A2111–A2154, 2013.

[60] S. Onori, P. Spagnol, V. Marano, Y. Guezennec, and G. Rizzoni, "A new life estimation method for lithium-ion batteries in plug-in hybrid electric vehicles applications," *International Journal of Power Electronics*, vol. 4, no. 3, pp. 302–319, 2012.

[61] M. Klett, R. Eriksson, J. Groot, P. Svens, K. C. Högström, R. W. Lindström, H. Berg, T. Gustafson, G. Lindbergh, and K. Edström, "Non-uniform aging of cycled commercial LiFePO4//graphite cylindrical cells revealed by post-mortem analysis," *Journal of Power Sources*, vol. 257, pp. 126–137, 2014.

[62] R. Mingant, J. Bernard, and V. Sauvant-Moynot, "Novel state-of-health diagnostic method for Li-ion battery in service," *Applied energy*, vol. 183, pp. 390–398, 2016.

[63] J. Groot, M. Swierczynski, A. I. Stan, and S. K. Kær, "On the complex ageing characteristics of high-power LiFePO4/graphite battery cells cycled with high charge and discharge currents," *Journal of Power Sources*, vol. 286, pp. 475–487, 2015.

[64] E. Sarasketa-Zabala, E. Martinez-Laserna, M. Berecibar, I. Gandiaga, L. M. Rodriguez-Martinez, and I. Villarreal, "Realistic lifetime prediction approach for Li-ion batteries," *Applied energy*, vol. 162, pp. 839–852, 2016.

[65] L. C. Casals, B. A. García, F. Aguesse, and A. Iturrondobeitia, "Second life of electric vehicle batteries: relation between materials degradation and environmental impact," *The International Journal of Life Cycle Assessment*, vol. 22, no. 1, pp. 82–93, 2017.

[66] J. Bi, T. Zhang, H. Yu, and Y. Kang, "State-of-health estimation of lithium-ion battery packs in electric vehicles based on genetic resampling particle filter," *Applied energy*, vol. 182, pp. 558–568, 2016.

[67] J. Cannarella and C. B. Arnold, "Stress evolution and capacity fade in constrained lithium-ion pouch cells," *Journal of Power Sources*, vol. 245, pp. 745–751, 2014.

[68] P. L. Moss, G. Au, E. J. Plichta, and J. P. Zheng, "Study of capacity fade of lithium-ion polymer rechargeable batteries with continuous cycling," *Journal of the Electrochemical Society*, vol. 157, no. 1, pp. A1–A7, 2010.

[69] K. Maher and R. Yazami, "A study of lithium ion batteries cycle aging by thermodynamics techniques," *Journal of Power Sources*, vol. 247, pp. 527–533, 2014.

[70] D. Ciechanowicz, A. Knoll, P. Osswald, and D. Pelzer, "Towards a business case for vehicle-to-gridmaximizing profits in ancillary service markets," in *Plug In Electric Vehicles in Smart Grids*. Springer, 2015, pp. 203–231.

[71] T. Lehtola and A. Zahedi, "Cost of EV battery wear due to vehicle to grid application," in *2015 Australasian Universities Power Engineering Conference (AUPEC)*. IEEE, 2015, pp. 1–4.

[72] M. Ouyang, X. Feng, X. Han, L. Lu, Z. Li, and X. He, "A dynamic capacity degradation model and its applications considering varying load for a large format Li-ion battery," *Applied energy*, vol. 165, pp. 48–59, 2016.

[73] A. Santos, N. McGuckin, H. Y. Nakamoto, D. Gray, and S. Liss, "Summary of travel trends: 2009 national household travel survey," National Household Travel Survey, Tech. Rep., 2011.

[74] R. R. Nejad, S. M. Hakimi, and S. M. Moghaddas Tafreshi, "Smart virtual energy storage control strategy to cope with uncertainties and increase renewable energy penetration," *Journal of Energy Storage*, vol. 6, pp. 80–94, 2016.

[75] M. Marinelli, S. Martinenas, K. Knezović, and P. B. Andersen, "Validating a centralized approach to primary frequency control with series-produced electric vehicles," *Journal of Energy Storage*, vol. 7, pp. 63–73, 2016.

[76] H. Mahmood, D. Michaelson, and J. Jiang, "Strategies for independent deployment and autonomous control of PV and battery units in islanded microgrids," *IEEE Journal of Emerging and Selected Topics in Power Electronics*, vol. 3, no. 3, pp. 742–755, 2015.

[77] A. Ahmadian, M. Sedghi, A. Elkamel, M. Fowler, and M. A. Golkar, "Plug-in electric vehicle batteries degradation modeling for smart grid studies: review, assessment and conceptual framework," *Renewable and Sustainable Energy Reviews*, vol. 81, pp. 2609–2624, 2018.

[78] M. Bayati, M. Abedi, H. Hosseinian, and G. B. Gharehpetian, "A novel control strategy for Reflex-based electric vehicle charging station with grid support functionality," *Journal of Energy Storage*, vol. 12, pp. 108–120, 2017.

[79] B. Vulturescu, S. Butterbach, and C. Forgez, "Experimental considerations on the battery lifetime of a hybrid power source made of ultracapacitors and lead-acid batteries," *IEEE Journal of Emerging and Selected Topics in Power Electronics*, vol. 2, no. 3, pp. 701–709, 2014.

[80] J. Han, S. K. Solanki, and J. Solanki, "Coordinated predictive control of a wind/battery microgrid system," *IEEE Journal of emerging and selected topics in power electronics*, vol. 1, no. 4, pp. 296–305, 2013.

[81] G. Lacey, T. Jiang, G. Putrus, and R. Kotter, "The effect of cycling on the state of health of the electric vehicle battery," in *2013 48th International Universities' Power Engineering Conference (UPEC)*. IEEE, 2013, pp. 1–7.

[82] D. Anseán, M. Dubarry, A. Devie, B. Y. Liaw, V. M. García, J. C. Viera, and M. González, "Operando lithium plating quantification and early detection of a commercial LiFePO4 cell cycled under dynamic driving schedule," *Journal of Power Sources*, vol. 356, pp. 36–46, 2017.

[83] C. P. Grey and J. M. Tarascon, "Sustainability and in situ monitoring in battery development," *Nature materials*, vol. 16, no. 1, p. 45, 2017.

[84] E. Chemali, M. Preindl, P. Malysz, and A. Emadi, "Electrochemical and electrostatic energy storage and management systems for electric drive vehicles: state-of-the-art review and future trends," *IEEE Journal of Emerging and Selected Topics in Power Electronics*, vol. 4, no. 3, pp. 1117–1134, 2016.

[85] M. Broussely, S. Herreyre, P. Biensan, P. Kasztejna, K. Nechev, and R. J. Staniewicz, "Aging mechanism in Li ion cells and calendar life predictions," *Journal of Power Sources*, vol. 97, pp. 13–21, 2001.

[86] M. Broussely, P. Biensan, F. Bonhomme, P. Blanchard, S. Herreyre, K. Nechev, and R. J. Staniewicz, "Main aging mechanisms in Li ion batteries," *Journal of power sources*, vol. 146, no. 1-2, pp. 90–96, 2005.

[87] J. Vetter, P. Novák, M. R. Wagner, C. Veit, K.-C. Möller, J. O. Besenhard, M. Winter, M. Wohlfahrt-Mehrens, C. Vogler, and A. Hammouche, "Ageing mechanisms in lithium-ion batteries," *Journal of power sources*, vol. 147, no. 1-2, pp. 269–281, 2005.

[88] C. Zhu, F. Lu, H. Zhang, and C. C. Mi, "Robust predictive battery thermal management strategy for connected and automated hybrid electric vehicles based on thermoelectric parameter uncertainty," *IEEE Journal of Emerging and Selected Topics in Power Electronics*, vol. 6, no. 4, pp. 1796–1805, 2018.

[89] K. L. Gering, S. V. Sazhin, D. K. Jamison, C. J. Michelbacher, B. Y. Liaw, M. Dubarry, and M. Cugnet, "Investigation of path dependence in commercial lithium-ion cells chosen for plug-in hybrid vehicle duty cycle protocols," *Journal of Power Sources*, vol. 196, no. 7, pp. 3395–3403, 2011.

[90] G. Sarre, P. Blanchard, and M. Broussely, "Aging of lithium-ion batteries," *Journal of power sources*, vol. 127, no. 1-2, pp. 65–71, 2004.

[91] T. Sasaki, T. Nonaka, H. Oka, C. Okuda, Y. Itou, Y. Kondo, Y. Takeuchi, Y. Ukyo, K. Tatsumi, and S. Muto, "Capacity-fading

mechanisms of LiNiO2-based lithium-ion batteries I. analysis by electrochemical and spectroscopic examination," *Journal of The Electrochemical Society*, vol. 156, no. 4, pp. A289–A293, 2009.

[92] J. Shim, R. Kostecki, T. Richardson, X. Song, and K. A. Striebel, "Electrochemical analysis for cycle performance and capacity fading of a lithium-ion battery cycled at elevated temperature," *Journal of power sources*, vol. 112, no. 1, pp. 222–230, 2002.

[93] J. Shim and K. A. Striebel, "Characterization of high-power lithium-ion cells during constant current cycling: part I. cycle performance and electrochemical diagnostics," *Journal of power sources*, vol. 122, no. 2, pp. 188–194, 2003.

[94] R. B. Wright, J. P. Christophersen, C. G. Motloch, J. R. Belt, C. D. Ho, V. S. Battaglia, J. A. Barnes, T. Q. Duong, and R. A. Sutula, "Power fade and capacity fade resulting from cycle-life testing of advanced technology development program lithium-ion batteries," *Journal of Power Sources*, vol. 119, pp. 865–869, 2003.

[95] Y. Zhang and C.-Y. Wang, "Cycle-life characterization of automotive lithium-ion batteries with LiNiO2 cathode," *Journal of the Electrochemical Society*, vol. 156, no. 7, pp. A527–A535, 2009.

[96] R. B. Wright, C. G. Motloch, J. R. Belt, J. P. Christophersen, C. D. Ho, R. A. Richardson, I. Bloom, S. A. Jones, V. S. Battaglia, and G. L. Henriksen, "Calendar-and cycle-life studies of advanced technology development program generation 1 lithium-ion batteries," *Journal of power sources*, vol. 110, no. 2, pp. 445–470, 2002.

[97] K. Amine, C. H. Chen, J. Liu, M. Hammond, A. Jansen, D. Dees, I. Bloom, D. Vissers, and G. Henriksen, "Factors responsible for impedance rise in high power lithium ion batteries," *Journal of power sources*, vol. 97, pp. 684–687, 2001.

[98] I. Bloom, B. W. Cole, J. J. Sohn, S. A. Jones, E. G. Polzin, V. S. Battaglia, G. L. Henriksen, C. Motloch, R. Richardson, and T. Unkelhaeuser, "An accelerated calendar and cycle life study of Li-ion cells," *Journal of Power Sources*, vol. 101, no. 2, pp. 238–247, 2001.

[99] I. Bloom, S. A. Jones, E. G. Polzin, V. S. Battaglia, G. L. Henriksen, C. G. Motloch, R. B. Wright, R. G. Jungst, H. L. Case, and D. H. Doughty, "Mechanisms of impedance rise in high-power, lithium-ion cells," *Journal of power sources*, vol. 111, no. 1, pp. 152–159, 2002.

[100] J. P. Christophersen, C. G. Motloch, C. D. Ho, D. F. Glenn, R. B. Wright, J. R. Belt, T. C. Murphy, and T. Q. Duong, "DOE Advanced technology development program for lithium-ion batteries: INEEL Interim report for Gen 2 cycle-life testing," Idaho National Engineering and Environmental Laboratory, Tech. Rep., 2002.

[101] X. Zhang, P. N. Ross, R. Kostecki, F. Kong, S. Sloop, J. B. Kerr, K. Striebel, E. J. Cairns, and F. McLarnon, "Diagnostic characterization of high power lithium-ion batteries for use in hybrid electric vehicles," *Journal of The Electrochemical Society*, vol. 148, no. 5, pp. A463–A470, 2001.

[102] M. Kassem, J. Bernard, R. Revel, S. Pelissier, F. Duclaud, and C. Delacourt, "Calendar aging of a graphite/LiFePO4 cell," *Journal of Power Sources*, vol. 208, pp. 296–305, 2012.

[103] Q. Zhang, S.-Z. Huang, J. Jin, J. Liu, Y. Li, H.-E. Wang, L.-H. Chen, B.-J. Wang, and B.-L. Su, "Engineering 3D bicontinuous hierarchically macro-mesoporous LiFePO 4/C nanocomposite for lithium storage with high rate capability and long cycle stability," *Scientific reports*, vol. 6, p. 25942, 2016.

[104] D. Aurbach, B. Markovsky, Y. Talyossef, G. Salitra, H.-J. Kim, and S. Choi, "Studies of cycling behavior, ageing, and interfacial reactions of LiNi0. 5Mn1. 5O4 and carbon electrodes for lithium-ion 5-V cells," *Journal of Power Sources*, vol. 162, no. 2, pp. 780–789, 2006.

[105] R. Ahmed, M. El Sayed, I. Arasaratnam, J. Tjong, and S. Habibi, "Reduced-order electrochemical model parameters identification and SOC estimation for healthy and aged Li-ion batteries part I: parameterization model development for healthy batteries," *IEEE journal of emerging and selected topics in power electronics*, vol. 2, no. 3, pp. 659–677, 2014.

[106] ——, "Reduced-order electrochemical model parameters identification and state of charge estimation for healthy and aged Li-ion batteriespart II: aged battery model and state of charge estimation," *IEEE Journal of Emerging and Selected Topics in Power Electronics*, vol. 2, no. 3, pp. 678–690, 2014.

[107] J.-W. Lee, Y. K. Anguchamy, and B. N. Popov, "Simulation of charge–discharge cycling of lithium-ion batteries under low-earth-orbit conditions," *Journal of Power Sources*, vol. 162, no. 2, pp. 1395–1400, 2006.

[108] J. Schmalstieg, S. Käbitz, M. Ecker, and D. U. Sauer, "From accelerated aging tests to a lifetime prediction model: analyzing lithium-ion batteries," in *2013 World Electric Vehicle Symposium and Exhibition (EVS27)*. IEEE, 2013, pp. 1–12.

[109] M. Dubarry, V. Svoboda, R. Hwu, and B. Y. Liaw, "Capacity loss in rechargeable lithium cells during cycle life testing: the importance of determining state-of-charge," *Journal of Power Sources*, vol. 174, no. 2, pp. 1121–1125, 2007.

[110] U. Tröltzsch, O. Kanoun, and H.-R. Tränkler, "Characterizing aging effects of lithium ion batteries by impedance spectroscopy," *Electrochimica Acta*, vol. 51, no. 8-9, pp. 1664–1672, 2006.

[111] S. S. Choi and H. S. Lim, "Factors that affect cycle-life and possible degradation mechanisms of a Li-ion cell based on LiCoO2," *Journal of Power Sources*, vol. 111, no. 1, pp. 130–136, 2002.

[112] K. Takei, K. Kumai, Y. Kobayashi, H. Miyashiro, N. Terada, T. Iwahori, and T. Tanaka, "Cycle life estimation of lithium secondary battery by extrapolation method and accelerated aging test," *Journal of Power Sources*, vol. 97, pp. 697–701, 2001.

[113] L. W. Juang, P. J. Kollmeyer, A. E. Anders, T. M. Jahns, R. D. Lorenz, and D. Gao, "Investigation of the influence of superimposed AC current on lithium-ion battery aging using statistical design of experiments," *Journal of Energy Storage*, vol. 11, pp. 93–103, 2017.

[114] I. Bloom, S. A. Jones, V. S. Battaglia, G. L. Henriksen, J. P. Christophersen, R. B. Wright, C. D. Ho, J. R. Belt, and C. G. Motloch, "Effect of cathode composition on capacity fade, impedance rise and power fade in high-power, lithium-ion cells," *Journal of power sources*, vol. 124, no. 2, pp. 538–550, 2003.

[115] I. Bloom, J. Christophersen, and K. Gering, "Differential voltage analyses of high-power lithium-ion cells: 2. Applications," *Journal of Power Sources*, vol. 139, no. 1-2, pp. 304–313, 2005.

[116] I. Bloom, J. P. Christophersen, D. P. Abraham, and K. L. Gering, "Differential voltage analyses of high-power lithium-ion cells: 3. Another anode phenomenon," *Journal of power sources*, vol. 157, no. 1, pp. 537–542, 2006.

[117] I. Bloom, B. G. Potter, C. S. Johnson, K. L. Gering, and J. P. Christophersen, "Effect of cathode composition on impedance rise in high-power lithium-ion cells: long-term aging results," *Journal of power sources*, vol. 155, no. 2, pp. 415–419, 2006.

[118] M. Dubarry and B. Y. Liaw, "Identify capacity fading mechanism in a commercial LiFePO4 cell," *Journal of Power Sources*, vol. 194, no. 1, pp. 541–549, 2009.

[119] K. Bellache, M. B. Camara, and B. Dakyo, "Transient power control for diesel-generator assistance in electric boat applications using supercapacitors and batteries," *IEEE Journal of Emerging and Selected Topics in Power Electronics*, vol. 6, no. 1, pp. 416–428, 2017.

[120] K. Amine, J. Liu, and I. Belharouak, "High-temperature storage and cycling of C-LiFePO4/graphite Li-ion cells," *Electrochemistry communications*, vol. 7, no. 7, pp. 669–673, 2005.

[121] D. Aurbach, B. Markovsky, A. Rodkin, E. Levi, Y. S. Cohen, H.-J. Kim, and M. Schmidt, "On the capacity fading of LiCoO2 intercalation electrodes:: the effect of cycling, storage, temperature, and surface film forming additives," *Electrochimica Acta*, vol. 47, no. 27, pp. 4291–4306, 2002.

[122] L. Lam and P. Bauer, "Practical capacity fading model for Li-ion battery cells in electric vehicles," *IEEE transactions on power electronics*, vol. 28, no. 12, pp. 5910–5918, 2012.

[123] A. Hoke, A. Brissette, K. Smith, A. Pratt, and D. Maksimovic, "Accounting for lithium-ion battery degradation in electric vehicle charging optimization," *IEEE Journal of Emerging and Selected Topics in Power Electronics*, vol. 2, no. 3, pp. 691–700, 2014.

[124] K. Liu, J. Wang, T. Yamamoto, and T. Morikawa, "Modelling the multilevel structure and mixed effects of the factors influencing the energy consumption of electric vehicles," *Applied energy*, vol. 183, pp. 1351–1360, 2016.

[125] J. S. Neubauer, E. Wood, and A. Pesaran, "A second life for electric vehicle batteries: answering questions on battery degradation and value," *SAE International Journal of Materials and Manufacturing*, vol. 8, no. 2, pp. 544–553, 2015.

[126] M. Dubarry, A. Devie *et al.*, "Battery cycling and calendar aging: year one testing results." University of Central Florida. Electric Vehicle Transportation Center (EVTC), Tech. Rep., 2016.

[127] S. Brown, K. Ogawa, Y. Kumeuchi, S. Enomoto, M. Uno, H. Saito, Y. Sone, D. Abraham, and G. Lindbergh, "Cycle life evaluation of 3 Ah LixMn2O4-based lithium-ion secondary cells for low-earth-orbit satellites: I. Full cell results," *Journal of Power Sources*, vol. 185, no. 2, pp. 1444–1453, 2008.

[128] J. R. Belt, C. D. Ho, T. J. Miller, M. A. Habib, and T. Q. Duong, "The effect of temperature on capacity and power in cycled lithium ion batteries," *Journal of power sources*, vol. 142, no. 1-2, pp. 354–360, 2005.

[129] S.-W. Eom, M.-K. Kim, I.-J. Kim, S.-I. Moon, Y.-K. Sun, and H.-S. Kim, "Life prediction and reliability assessment of lithium secondary batteries," *Journal of Power Sources*, vol. 174, no. 2, pp. 954–958, 2007.
[130] K. Smith, M. Warleywine, E. Wood, J. Neubauer, and A. Pesaran, "Comparison of plug-in hybrid electric vehicle battery life across geographies and drive-cycles," National Renewable Energy Lab.(NREL), Golden, CO (United States), Tech. Rep., 2012.
[131] J. S. Neubauer and E. Wood, "Will your battery survive a world with fast chargers?" SAE Technical Paper, Tech. Rep., 2015.
[132] S.-Y. Liong, W.-H. Lim, and G. N. Paudyal, "River stage forecasting in Bangladesh: neural network approach," *Journal of computing in civil engineering*, vol. 14, no. 1, pp. 1–8, 2000.
[133] A. Kordjazi, F. Pooya Nejad, and M. B. Jaksa, "Prediction of load-carrying capacity of piles using a support vector machine and improved data collection," in *12th Australia New Zealand Conference on Geomechanics (ANZ 2015)*. The New Zealand Geotechnical Society and the Australian Geomechanics Society, Feb. 2015, pp. 1–8.
[134] G. Mills and I. MacGill, "Assessing electric vehicle storage, flexibility, and distributed energy resource potential," *Journal of Energy Storage*, vol. 17, pp. 357–366, 2018.

Timo A. Lehtola is born in Finland and holds a masters degree in Energy Technology from the Lappeenranta University of Technology and a masters degree in Physics from the University of Helsinki.

He is a Ph.D. student at the James Cook University, Australia. Previous publications include a review article in Sustainable Energy Technologies and Assessments in 2019, titled Solar energy and wind power supply supported by storage technology: A review. Previous research interests include battery management and peak demand management in grid-connected electric vehicles and distributed renewable energy generation systems.

Mr. Lehtola is a member of IEEE, IEEE Young Professionals, Cigr, Cigr Next Generation Network, and IEEE Power & Energy Society. He has received IEEE PES Queensland Travel Award in 2016.

Associate Professor Ahmad Zahedi is with the college of Science, Technology, and Engineering of James Cook University, Queensland, Australia.

Educated in Iran and Germany, Ahmad is author or co-author of more than 180 publications including 4 books and has trained 20 postgraduate candidates at PhD and Master Levels, has examined more than 50 PhD and Master Thesis, and completed 15 research and industry-funded projects. Ahmad has 26 years tertiary teaching and research and 6 years industry experience.